ISSN 2644-3260 (online)

Artificial Intelligence in *Medical Imaging*

Artif Intell Med Imaging 2020 August 28; 1(2): 70-86

Published by Baishideng Publishing Group Inc

AIMI

Artificial Intelligence in Medical Imaging

Contents

Bimonthly Volume 1 Number 2 August 28, 2020

MINIREVIEWS

Contents

ABOUT COVER

Co-Editor-in-Chief of *Artificial Intelligence in Medical Imaging*, Dr Ahmed Abdel Khalek Abdel Razek, MD is Professor and Head of the Diagnostic Radiology Department, Faculty of Medicine, Mansoura University (Egypt). He has published more than 200 papers as lead author in peer-reviewed, high-impact journals. He has written four book chapters and presented more than 400 papers at national and international congresses. He serves as reviewer for more than 100 high-impact journals and as an editorial board member of 7 peer-reviewed journals. He has supervised more than 100 PhD and MD thesis students. His research involves head and neck imaging, neuroradiology and advanced magnetic resonance imaging techniques, such as diffusion, perfusion, and magnetic resonance spectroscopy, including studies on artificial intelligence and deep learning in the field of medical imaging. He has won scientific awards from Scopus, Publons, the Radiological Society of North America, and the European Society of Radiology. (L-Editor: Filipodia)

AIMS AND SCOPE

The primary aim of *Artificial Intelligence in Medical Imaging* (*AIMI*, *Artif Intell Med Imaging*) is to provide scholars and readers from various fields of artificial intelligence in medical imaging with a platform to publish high-quality basic and clinical research articles and communicate their research findings online.

AIMI mainly publishes articles reporting research results obtained in the field of artificial intelligence in medical imaging and covering a wide range of topics, including artificial intelligence in radiology, pathology image analysis, endoscopy, molecular imaging, and ultrasonography.

INDEXING/ABSTRACTING

There is currently no indexing.

RESPONSIBLE EDITORS FOR THIS ISSUE

Production Editor: *Yan-Xia Xing*; **Production Department Director:** *Yun-Xiaojian Wu*; **Editorial Office Director:** *Jin-Lei Wang*.

NAME OF JOURNAL
Artificial Intelligence in Medical Imaging

ISSN
ISSN 2644-3260 (online)

LAUNCH DATE
June 28, 2020

FREQUENCY
Bimonthly

EDITORS-IN-CHIEF
Xue-Li Chen, Caroline Chung, Ahmed Abdel Khalek Abdel Razek, Jun Shen

EDITORIAL BOARD MEMBERS
https://www.wjgnet.com/2644-3260/editorialboard.htm

PUBLICATION DATE
August 28, 2020

INSTRUCTIONS TO AUTHORS
https://www.wjgnet.com/bpg/gerinfo/204

GUIDELINES FOR ETHICS DOCUMENTS
https://www.wjgnet.com/bpg/GerInfo/287

GUIDELINES FOR NON-NATIVE SPEAKERS OF ENGLISH
https://www.wjgnet.com/bpg/gerinfo/240

PUBLICATION ETHICS
https://www.wjgnet.com/bpg/GerInfo/288

PUBLICATION MISCONDUCT
https://www.wjgnet.com/bpg/gerinfo/208

ARTICLE PROCESSING CHARGE
https://www.wjgnet.com/bpg/gerinfo/242

STEPS FOR SUBMITTING MANUSCRIPTS
https://www.wjgnet.com/bpg/GerInfo/239

ONLINE SUBMISSION
https://www.f6publishing.com

Artificial Intelligence in Medical Imaging

Submit a Manuscript: https://www.f6publishing.com

Artif Intell Med Imaging 2020 August 28; 1(2): 70-77

DOI: 10.35711/aimi.v1.i2.70

ISSN 2644-3260 (online)

MINIREVIEWS

Artificial intelligence and pituitary adenomas: A review

Elvira Guerriero, Lorenzo Ugga, Renato Cuocolo

ORCID number: Elvira Guerriero 0000-0003-3853-721X; Lorenzo Ugga 0000-0001-7811-4612; Renato Cuocolo 0000-0002-1452-1574.

Author contributions: Guerriero E collected the data and wrote the paper; Ugga L collected the data and edited the paper; Cuocolo R collected the data and edited the paper.

Conflict-of-interest statement: No conflict of interest.

Manuscript source: Invited manuscript

Received: May 25, 2020
Peer-review started: May 25, 2020
First decision: July 4, 2020
Revised: July 15, 2020
Accepted: August 22, 2020
Article in press: August 22, 2020

Elvira Guerriero, Lorenzo Ugga, Renato Cuocolo, Department of Advanced Biomedical Sciences, University of Naples "Federico II", Naples 80131, Italy

Corresponding author: Renato Cuocolo, MD, PhD, Department of Advanced Biomedical Sciences, University of Naples "Federico II", via Pansini 5, Naples 80131, Italy. renato.cuocolo@unina.it

Abstract

The aim of this review was to provide an overview of the main concepts in machine learning (ML) and to analyze the ML applications in the imaging of pituitary adenomas. After describing the clinical, pathological and imaging features of pituitary tumors, we defined the difference between ML and classical rule-based algorithms, we illustrated the fundamental ML techniques: supervised, unsupervised and reinforcement learning and explained the characteristic of deep learning, a ML approach employing networks inspired by brain's structure. Pre-treatment assessment and neurosurgical outcome prediction were the potential ML applications using magnetic resonance imaging. Regarding pre-treatment assessment, ML methods were used to have information about tumor consistency, predict cavernous sinus invasion and high proliferative index, discriminate null cell adenomas, which respond to neo-adjuvant radiotherapy from other subtypes, predict somatostatin analogues response and visual pathway injury. Regarding neurosurgical outcome prediction, the following applications were discussed: Gross total resection prediction, evaluation of Cushing disease recurrence after transsphenoidal surgery and prediction of cerebrospinal fluid fistula's formation after surgery. Although clinical applicability requires more replicability, generalizability and validation, results are promising, and ML software can be a potential power to facilitate better clinical decision making in pituitary tumor patients.

Key Words: Pituitary adenoma; Machine learning; Deep learning; Radiomics; Texture analysis; Magnetic resonance imaging

Core Tip: Machine learning (ML) has seen an explosion of interest in medical imaging because of its capability of analyzing large amounts of data. Recent studies applied ML techniques to the imaging of pituitary adenomas. The purpose of our review was to describe the main concepts in ML and its current and potential applications in imaging

Published online: August 28, 2020

P-Reviewer: Wang RF
S-Editor: Wang JL
L-Editor: A
P-Editor: Xing YX

analysis of pituitary tumors.

Citation: Guerriero E, Ugga L, Cuocolo R. Artificial intelligence and pituitary adenomas: A review. *Artif Intell Med Imaging* 2020; 1(2): 70-77
URL: https://www.wjgnet.com/2644-3260/full/v1/i2/70.htm
DOI: https://dx.doi.org/10.35711/aimi.v1.i2.70

INTRODUCTION

Pituitary adenomas are benign tumors accounting for 15%-20% of all intracranial neoplasms, with an incidence of 80–90 cases per 100000 population[1,2]. Microadenomas are defined as tumors < 10 mm in maximum diameter, whereas larger adenomas are considered macroadenomas. Their peak age of presentation is between the fourth and seventh decades. Almost two-thirds of pituitary adenomas are hormone-secreting, prolactin most commonly, followed by growth hormone, corticotropin and thyrotropin, and cause typical hypersecretion syndromes. Non-functioning, small intrasellar tumors can be clinically silent and diagnosed only as incidental magnetic resonance findings, while bulky pituitary macroadenomas typically present with mass effect signs, such as headache, visual disturbances, and hypopituitarism[3,4]. The 2017 World Health Organization (WHO) classification adopted pituitary adenohypophyseal cell lineage as the main principle guiding the classification of adenomas. According to this principle we distinguish the acidophilic lineage (in which the involved transcription factor is PIT1), the corticotrope lineage (TPIT transcription factor), and the gonadotroph lineage (SF1 transcription factor). Null-cell adenomas (NCAs) are now defined as tumors that have no immunohistochemical evidence of cell-type-specific differentiation considering both pituitary hormones and transcription factors. Furthermore, in the new WHO classification the term "atypical adenoma" has been abandoned and replaced by "high risk adenoma", in reference to tumors with high proliferation index and tendency to invasion. In particular, emphasis is placed on the evaluation of tumor proliferation (mitotic count and Ki-67 index), tumor invasion, and on special adenomas variants for which clinical behavior has been shown to be more aggressive due to their intrinsic histological features: lactotroph adenoma in men, sparsely granulated somatotroph adenoma, the silent corticotroph adenoma, the Crooke's cell adenoma and the plurihormonal PIT1-positive adenoma[5]. Magnetic resonance imaging (MRI) is the investigation of choice for a complete evaluation of pituitary adenomas[6]. Various parameters regarding the extent, consistency, and contrast enhancement can be analyzed in order to help neurosurgeons in planning an appropriate surgical approach and long-term follow-up[7].

Attempting to predict invasion (cavernous and/or sphenoid sinus involvement) based on imaging is an important challenge. The Knosp classification is one of the more commonly used systems to determine the likelihood of cavernous sinus invasion by pituitary macroadenomas, but the highest accuracy of this grading system is observed in extreme cases of overt invasion or non-invasion, while sensitivity and specificity are low in intermediate cases[8,9].

Tumor consistency in pituitary macroadenomas has been known to be one of the main factors that determine the success rate of the transsphenoidal approach. The role of MRI in predicting the consistency of pituitary macroadenomas is controversial. Several studies suggested that relative signal intensity or signal intensity ratio on T2-weighted MRI correlates with the tumor consistency, while some others concluded that they have no predictive value[10-12]. A similar controversy has been reported in several studies which investigated the usefulness of diffusion-weighted imaging in tumor consistency prediction[13-15].

Considering the above, it is still difficult to achieve an early identification of clinical and radiological features suggestive of an aggressive behavior, characterized by rapid growth, local invasion, and high ki-67 proliferation index.

In this setting, artificial intelligence (AI) has proved promising in recently published papers. Machine learning (ML) is a subfield of AI that employs algorithms to allow computers to learn directly from the data and subsequently perform predictions without explicit prior programming. The potential impact of ML on medicine, and particularly medical imaging, is relative to its ability to analyze large datasets including gray level textural features that humans do not consciously assess. Unlike

classical rule-based algorithms, machine learning can take advantage of increased exposure to new data and learn over time[16]. ML techniques can be further divided into supervised, unsupervised learning and reinforcement learning[17-20]. In supervised learning there is a ground truth which is directly used to guide the algorithm training process. The goal of the resulting model is usually to learn a general rule that maps inputs to outputs and is applicable to new, unseen cases. In unsupervised learning there is no preliminary labeling and therefore its goal is to cluster the given inputs based solely on the underlying data structure. Finally, reinforcement learning consists of a computer program performing an assigned task in a dynamic environment and consequently receiving feedback as a positive or negative reinforcement. To improve algorithm's performance, these approaches can be combined, some examples are semi-supervised, self-supervised and multi-instance learning.

Deep learning (DL) is an ML approach employing networks inspired by brain's structure, with a large number of simple interconnected units performing complicated tasks. The DL algorithms most applied to medical imaging are convolutional neural networks. Lower level information inputs, derived from imaging data transformed in feature vectors, form connections to the next level or "layer" of neurons. Each neuron in this second layer can combine the inputs from lower level neurons to form a newer, more complex output. As the number of intermediate or hidden layers increases, the final output from the highest layer becomes richer and more complex.

ML tasks are not limited to tumor property prediction but include many possible applications in other medical imaging and daily workflow fields, such as image acquisition, segmentation, image quality analytics, automated dose estimation and radiology reporting[21-23]. Despite the high number of recent ML successes, there are still many limitations in its clinical use[24-27]. First of all, an obstacle to AI adoption in the clinical setting is identifiable in its limited interpretability, especially true for DL. Clinicians are consequently reluctant to trust and to adopt something whose decision process is not fully understood. Secondly, ML research has to deal with issues due to the nature of the health domain, including the lack of large amounts of data, necessary during the training phase, the need for algorithm frequent updating and potential model overfitting.

This review aims to give an overview of the current applications of ML methods in pituitary adenomas evaluation.

PRETREATMENT ASSESSMENT

Tumor consistency is one of the main factors that determine the success-rate of transsphenoidal adenomectomy. For this reason, pre-operative information about tumor consistency would help neurosurgeons in planning the most appropriate surgical approach. Zeynalova *et al*[28] demonstrated the utility of ML-based histogram analysis (from 55 pituitary adenoma patients) to predict tumor consistency and compared it with a conventional signal intensity ratio (SIR) evaluation. Histogram features were extracted from coronal T2-weighted original, filtered and transformed MRI images by manual segmentation. The high dimensionality of the histogram texture features was reduced with reproducibility analysis, collinearity analysis and wrapper-based feature selection. They employed the artificial neural network (ANN) as ML classifier. The reference-standard was consensual evaluations of neurosurgeons and pathologists. For histogram analysis, the ANN correctly classified 72.5% of pituitary macroadenomas with an area under the receiver operating characteristic (ROC) curve (AUC) value of 0.710. As for SIR evaluation, accuracy and AUC values were 74.5% and 0.551, respectively. Considering AUC values, ML-based histogram analysis performed better than SIR evaluation[28].

Fan *et al*[29] demonstrated how a radiomics model can assist neurosurgeons in predicting tumor consistency in patients with acromegaly before surgery and facilitate the determination of an appropriate therapeutic approach. 158 patients (training group n = 100, validation group n = 58) were included in this retrospective study, while 30 were enrolled in a prospective multi-center study for model validation. The consistency of the tumor was classified as soft or firm according to the neurosurgeon's evaluation. All patients underwent MRI examination which included T1-, T2- and contrast-enhanced T1-weighted sequences in the coronal plane, used for feature extraction. The radiomics features were collected based on the regions of interest drawn by an expert neuroradiologist and verified by a second expert. Total 1561 quantitative features were collected for every sequence. The radiomics features were determined using the elastic net feature selection algorithm, and the radiomics

signature was constructed. Next, a radiomics model was developed using the radiomics signature and clinical characteristics, which were further screened according to the Akaike information criterion. Then, 30 patients with acromegaly from three hospitals were enrolled for multicenter validation of the model. The prediction accuracy was then evaluated through ROC analyses and associated classification measures. The radiomics model constructed in this study showed an AUC of 0.83 and 0.81 in the primary and validation cohorts, respectively. In conclusion, this model was convenient to use and could accurately predict the tumor consistency in a multicenter prospective validation before surgery[29].

The pre-operative prediction of cavernous sinus (CS) invasion by pituitary adenomas (Knosp grade 2-3) can help neurosurgeons in planning the surgical approach, follow-up, and long-term management. Niu *et al*[30] used a radiomics method to predict CS invasion, enrolling 194 patients with Knosp grade 2-3 (training set n = 97; test set n = 97) and extracting 2553 quantitative imaging texture features from contrast-enhanced T1- and T2-weighted MR images. A linear support vector machine (SVM) was used to fit the predictive model, then a nomogram was constructed incorporating radiomics signature and clinico-radiological risk factors. Radiomics model yielded an AUC of 0.852 and 0.826 for the training and test set, respectively. The nomogram yielded an AUC of 0.899 in the training test and 0.871 in the test set[30].

According to the 2017 WHO classification, "high risk" pituitary adenomas are tumors with rapid growth, radiological invasion, and high Ki-67 proliferation index. MRI had already proved promising in proliferative index prediction, using diffusion-weighted imaging. Indeed, Tamrazi *et al*[31] performed a retrospective review of diffusion imaging and immunohistochemical characteristics of 17 with pituitary macroadenomas and demonstrated an inverse relationship between apparent diffusion coeffcient values and Ki-67. In this context, machine learning can be effective for the early identification of "high risk" adenomas and could allow making a more accurate pre-operative assessment and long-term follow-up. Regarding the last, a recent study by Ugga *et al*[32] employed ML analysis of texture-derived parameters from pre-operative coronal T2-weighted MR images. A total of 89 patients that underwent endoscopic endonasal procedure were included. Pituitary adenomas were classified in high versus low Ki-67 proliferation index according to pathological data. Total 1128 features were extracted, and different supervised feature selection methods were employed to select the most informative features. A k-nearest neighbors (k-NN) classifier was used to predict the proliferative index, then algorithm validation was performed with a train-test approach. The accuracy of k-NN in the test group was 91.67% of correctly classified patients.

Non-functioning pituitary adenomas are a huge group of adenomas and can be divided in NCAs, oncocytomas and gonadotrophic adenomas. Patients with NCAs are more likely to respond to neo-adjuvant radiotherapy, so radiomics could play a role in discriminating preoperatively NCAs from other subtypes. Zhang *et al*[33] enrolled 112 patients (training set n = 75; test set n = 37) with non-functioning pituitary adenomas who underwent MR examination. In their retrospective study a SVM trained a predictive model that was validated using a ROC analysis on an independent test set. Then, a nomogram was constructed incorporating clinical characteristics and the radiomics signature for a more individualized predictive model. T1-weighted image features yielded an AUC value of 0.83 and 0.80 for the training and test sets, respectively. The nomogram incorporating sex and the T1 radiomics signature yielded good calibration in the training and test sets (concordance index of 0.854 and 0.857, respectively)[33].

Somatostatin analogues (SAs) response prediction is an essential information in acromegalic patient medical treatment in the presence of GH-secreting pituitary adenomas. Indeed, this medical treatment can improve the surgical outcome, but it is burdened by high costs. Heck *et al*[34] showed how quantitative analysis of T2-weighted MR images could predict response to SAs in patients with acromegaly. However, they verified that conventional visual T2 intensity assessment achieved similar results. This retrospective cohort study included 58 newly diagnosed patients. Parameters from the T2 histogram analyses (T2 intensity ratio and T2 homogeneity ratio) were correlated to visually assessed T2 intensity (hypo-, iso- or hyperintense), baseline characteristics, response to SA treatment, and histological granulation pattern (anti-Cam5.2). T2 intensity ratio was lowest in the hypointense tumors and highest in the hyperintense tumors. T2 intensity at baseline correlated with reduction in GH (r = -0.67) and IGF-1 (r = -0.36) after primary SA treatment (n = 34). The T2 homogeneity ratio correlated with adenoma size reduction (r = -0.45). Sparsely granulated adenomas, which are typically associated to resistance to SAs, had a higher T2 intensity than densely or intermediately granulated adenomas. In conclusion, using T2 histogram analyses the

authors found that high T2 intensity correlated with more aggressive adenoma subtypes, larger adenoma size, lower GH and IGF-1 production, and blunted response to an octreotide test dose at baseline. Moreover, a better biochemical response to SA therapy was observed in adenomas with low T2 intensity. In their retrospective study, Kocak *et al*[35] demonstrated the potential role of ML-based high-dimensional quantitative texture analysis (qTA) in predicting SAs response in acromegalic patients with a GH-secreting pituitary adenoma. They showed how ML performs better than relative signal intensity (rSI) evaluation or immunohistochemical granulation pattern evaluation. Coronal T2-weighted images of 47 patients (24 SA responsive and 23 SA resistant patients) were used for qTA and quantitative and qualitative rSI evaluation, while the immunohistochemical evaluation was based on the granulation pattern of the adenomas. ML classifiers were k-NN and C4.5 algorithm. The reference standard was the biochemical response status (6 months post-therapy). Predictive performance of qTA was compared with that of the quantitative and qualitative rSI and immunohistochemical evaluation. For the qTA, k-NN correctly classified 85.1% macroadenomas with an AUC of 0.847. The accuracy and AUC ranges of the other methods were lower, equal to 57.4/70.2% and 0.575/0.704, respectively[35].

Pituitary tumor growth can lead to compression of the anterior visual pathways, leading to visual impairment, which is the most common and earliest symptom in this pathology. In their retrospective study Lilja *et al*[36] demonstrated that diffusion Tensor imaging (DTI) and a prediction model may be an additional diagnostic tool that provides objective data about visual pathway injury, guiding treatment decisions. Total 23 patients with pituitary adenomas and 20 healthy patients underwent a complete neuro-ophthalmological examination and an MRI study, which included 3D T1-weighted and DTI sequences. A prediction model using logistic regression was constructed to test the capability of DTI parameters to correctly classify a subject as a patient (before surgery) or a control. Total 12 features quantifying mean DTI parameters from the optic tract regions were included. Based on the axial diffusivity and fractional anisotropy, the prediction model could separate patients from controls with high sensitivity. The prediction model correctly classified all patients with visual field defects (sensitivity = 1.0), 9 of 12 patients without visual field defects (sensitivity = 0.75), and 17 of 20 controls (specificity = 0.85)[36].

NEUROSURGICAL OUTCOME PREDICTION

Gross total resection (GTR) is the main surgical goal in transsphenoidal surgery for most pituitary adenomas. Predictive analytics for GTR may help in surgical decision-making, especially in intermediate cases (Knops grade 2-3A). In their retrospective study, Staartjes *et al*[37] investigated the potential value of deep neural network for predicting GTR in comparison with the Knops classification and logistic regression. They enrolled a total of 140 patients who underwent endoscopic transsphenoidal surgery and trained a deep neural network to predict GTR from 16 preoperatively available neuro-radiological and procedural variables. Their DL model (AUC = 0.96; accuracy = 91%; sensitivity = 94%; specificity = 89%) outperformed both the Knosp classification (AUC = 0.87; accuracy = 81%; sensitivity = 92%; specificity = 70%) and logistic regression (AUC = 0.86; accuracy = 82%; sensitivity = 81%; specificity = 83%)[37].

In their retrospective study, Liu *et al*[38] aimed to develop machine learning-based predictive models to evaluate Cushing disease recurrence after initial transsphenoidal surgery and to investigate their performance. Seventeen radiomic features including tumor volume computed from pre-operative MRI (contrast-enhanced T1-weighted MRI) and other pre/post-operative clinical variables were evaluated. Five supervised ML algorithms, including decision tree, gradient boosting decision tree, random forest (RF), adaptive boosting, and extreme gradient boost and 2 conventional models (Logistic regression, Naïve Bayes) were applied. Models were evaluated based on their AUC. The study demonstrated that ML-based predictive models for neurosurgical outcomes performed well, better than some conventional models such as logistic regression. Using 17 variables, several ML-based predictive models for recurrence were developed, and most of them (4/5) maintained high performance, with AUCs ranging from 0.694 to 0.781 which were much higher than that of conventional statistics. The best performance (AUC = 0.781) was obtained introducing 8 variables to RF algorithm, which was much better than that of logistic regression (AUC = 0.684) and that of using only postoperative morning serum cortisol (AUC = 0.635). According to the feature selection algorithms, the top predictors were age, postoperative serum cortisol, and postoperative ACTH[38].

Cerebrospinal fluid (CSF) fistulas remain a major complication of transnasal transsphenoidal surgery for pituitary adenoma. Staartjes *et al*[39] developed a neural network–based model with the aim of classifying pituitary surgeries in having high versus low-risk of CSF leak. From a prospective registry, 154 patients who underwent endoscopic transnasal transsphenoidal surgery for pituitary adenoma were identified and underwent an MRI study. Moreover, risk factors for intraoperative CSF leaks were identified using conventional statistical methods. Selected features included both imaging features from inter-carotid distances and other clinical pre/post-operative variables. The authors built a predictive model for intraoperative CSF leaks based on a deep multilayer perceptron with 5 hidden layers. The deep neural network–based prediction model could identify patients at high risk for intraoperative CSF leak. It correctly classified 88% of patients in the test set, with an AUC of 0.84. Sensitivity and specificity were high, of 83% and 89% respectively. The positive predictive value was 71%, negative predictive value was 94%, and F1 score was 0.77[39].

CONCLUSION

We reviewed a set of articles related to ML applications in pituitary adenomas. These studies showed that ML has a certain potential to improve the diagnostic performance of MRI in pre-treatment assessment and neurosurgical outcome prediction. In current studies there is not a standardized procedure, ML methodologies vary a lot, different types of classifiers are applied and only a few models are validated on an external set. The major limits of these studies are the replicability and generalizability. Publicly available datasets are needed, and clinical applicability still requires more robust validation across different sites, scanner vendors and field intensity. However, the research in the years is growing rapidly and ML software can be a potential power to facilitate better clinical decision making in pituitary tumor patients.

REFERENCES

1 **McDowell BD**, Wallace RB, Carnahan RM, Chrischilles EA, Lynch CF, Schlechte JA. Demographic differences in incidence for pituitary adenoma. *Pituitary* 2011; **14**: 23-30 [PMID: 20809113 DOI: 10.1007/s11102-010-0253-4]

2 **Fernandez A**, Karavitaki N, Wass JA. Prevalence of pituitary adenomas: a community-based, cross-sectional study in Banbury (Oxfordshire, UK). *Clin Endocrinol (Oxf)* 2010; **72**: 377-382 [PMID: 19650784 DOI: 10.1111/j.1365-2265.2009.03667.x]

3 **Chen L**, White WL, Spetzler RF, Xu B. A prospective study of nonfunctioning pituitary adenomas: presentation, management, and clinical outcome. *J Neurooncol* 2011; **102**: 129-138 [PMID: 20730474 DOI: 10.1007/s11060-010-0302-x]

4 **Asa SL**, Ezzat S. The pathogenesis of pituitary tumors. *Annu Rev Pathol* 2009; **4**: 97-126 [PMID: 19400692 DOI: 10.1146/annurev.pathol.4.110807.092259]

5 **Inoshita N**, Nishioka H. The 2017 WHO classification of pituitary adenoma: overview and comments. *Brain Tumor Pathol* 2018; **35**: 51-56 [PMID: 29687298 DOI: 10.1007/s10014-018-0314-3]

6 **Gupta K**, Sahni S, Saggar K, Vashisht G. Evaluation of Clinical and Magnetic Resonance Imaging Profile of Pituitary Macroadenoma: A Prospective Study. *J Nat Sci Biol Med* 2018; **9**: 34-38 [PMID: 29456390 DOI: 10.4103/jnsbm.JNSBM_111_17]

7 **Boxerman JL**, Rogg JM, Donahue JE, Machan JT, Goldman MA, Doberstein CE. Preoperative MRI evaluation of pituitary macroadenoma: imaging features predictive of successful transsphenoidal surgery. *AJR Am J Roentgenol* 2010; **195**: 720-728 [PMID: 20729452 DOI: 10.2214/AJR.09.4128]

8 **Knosp E**, Steiner E, Kitz K, Matula C. Pituitary adenomas with invasion of the cavernous sinus space: a magnetic resonance imaging classification compared with surgical findings. *Neurosurgery* 1993; **33**: 610-7; discussion 617-8 [PMID: 8232800 DOI: 10.1227/00006123-199310000-00008]

9 **Micko AS**, Wöhrer A, Wolfsberger S, Knosp E. Invasion of the cavernous sinus space in pituitary adenomas: endoscopic verification and its correlation with an MRI-based classification. *J Neurosurg* 2015; **122**: 803-811 [PMID: 25658782 DOI: 10.3171/2014.12.JNS141083]

10 **Bahuleyan B**, Raghuram L, Rajshekhar V, Chacko AG. To assess the ability of MRI to predict consistency of pituitary macroadenomas. *Br J Neurosurg* 2006; **20**: 324-326 [PMID: 17129884 DOI: 10.1080/02688690601000717]

11 **Hagiwara A**, Inoue Y, Wakasa K, Haba T, Tashiro T, Miyamoto T. Comparison of growth hormone-producing and non-growth hormone-producing pituitary adenomas: imaging characteristics and pathologic correlation. *Radiology* 2003; **228**: 533-538 [PMID: 12819334 DOI: 10.1148/radiol.2282020695]

12 **Snow RB**, Johnson CE, Morgello S, Lavyne MH, Patterson RH Jr. Is magnetic resonance imaging useful in guiding the operative approach to large pituitary tumors? *Neurosurgery* 1990; **26**: 801-803 [PMID: 2352598 DOI: 10.1097/00006123-199005000-00011]

13 **Pierallini A**, Caramia F, Falcone C, Tinelli E, Paonessa A, Ciddio AB, Fiorelli M, Bianco F, Natalizi S, Ferrante L, Bozzao L. Pituitary macroadenomas: preoperative evaluation of consistency with diffusion-weighted MR imaging--initial experience. *Radiology* 2006; **239**: 223-231 [PMID: 16452397 DOI:

10.1148/radiol.2383042204]
14 **Mohamed FF**, Abouhashem S. Diagnostic value of apparent diffusion coefficient (ADC) in assessment of pituitary macroadenoma consistency. *Egypt J Radiol Nucl Med* 2013; **44**: 617–24 [DOI: 10.1016/j.ejrnm.2013.05.012]
15 **Suzuki C**, Maeda M, Hori K, Kozuka Y, Sakuma H, Taki W, Takeda K. Apparent diffusion coefficient of pituitary macroadenoma evaluated with line-scan diffusion-weighted imaging. *J Neuroradiol* 2007; **34**: 228-235 [PMID: 17719632 DOI: 10.1016/j.neurad.2007.06.007]
16 **Erickson BJ**, Korfiatis P, Akkus Z, Kline TL. Machine Learning for Medical Imaging. *Radiographics* 2017; **37**: 505-515 [PMID: 28212054 DOI: 10.1148/rg.2017160130]
17 **Choy G**, Khalilzadeh O, Michalski M, Do S, Samir AE, Pianykh OS, Geis JR, Pandharipande PV, Brink JA, Dreyer KJ. Current Applications and Future Impact of Machine Learning in Radiology. *Radiology* 2018; **288**: 318-328 [PMID: 29944078 DOI: 10.1148/radiol.2018171820]
18 **Wang S**, Summers RM. Machine learning and radiology. *Med Image Anal* 2012; **16**: 933-951 [PMID: 22465077 DOI: 10.1016/j.media.2012.02.005]
19 **Gillies RJ**, Kinahan PE, Hricak H. Radiomics: Images Are More than Pictures, They Are Data. *Radiology* 2016; **278**: 563-577 [PMID: 26579733 DOI: 10.1148/radiol.2015151169]
20 **Schmidt J**, Marques MRG, Botti S, Marques MAL. Recent advances and applications of machine learning in solid-state materials science. *NPJ Comput Mater* 2019; **5**: 83 [DOI: 10.1038/s41524-019-0221-0]
21 **Zaharchuk G**, Gong E, Wintermark M, Rubin D, Langlotz CP. Deep Learning in Neuroradiology. *AJNR Am J Neuroradiol* 2018; **39**: 1776-1784 [PMID: 29419402 DOI: 10.3174/ajnr.A5543]
22 **Mazurowski MA**, Buda M, Saha A, Bashir MR. Deep learning in radiology: An overview of the concepts and a survey of the state of the art with focus on MRI. *J Magn Reson Imaging* 2019; **49**: 939-954 [PMID: 30575178 DOI: 10.1002/jmri.26534]
23 **McBee MP**, Awan OA, Colucci AT, Ghobadi CW, Kadom N, Kansagra AP, Tridandapani S, Auffermann WF. Deep Learning in Radiology. *Acad Radiol* 2018; **25**: 1472-1480 [PMID: 29606338 DOI: 10.1016/j.acra.2018.02.018]
24 **Romeo V**, Ricciardi C, Cuocolo R, Stanzione A, Verde F, Sarno L, Improta G, Mainenti PP, D'Armiento M, Brunetti A, Maurea S. Machine learning analysis of MRI-derived texture features to predict placenta accreta spectrum in patients with placenta previa. *Magn Reson Imaging* 2019; **64**: 71-76 [PMID: 31102613 DOI: 10.1016/j.mri.2019.05.017]
25 **Ciompi F**, Chung K, van Riel SJ, Setio AAA, Gerke PK, Jacobs C, Scholten ET, Schaefer-Prokop C, Wille MMW, Marchianò A, Pastorino U, Prokop M, van Ginneken B. Towards automatic pulmonary nodule management in lung cancer screening with deep learning. *Sci Rep* 2017; **7**: 46479 [PMID: 28422152 DOI: 10.1038/srep46479]
26 **Cuocolo R**, Perillo T, De Rosa E, Ugga L, Petretta M. Current applications of big data and machine learning in cardiology. *J Geriatr Cardiol* 2019; **16**: 601-607 [PMID: 31555327 DOI: 10.11909/j.issn.1671-5411.2019.08.002]
27 **Islam MM**, Nasrin T, Walther BA, Wu CC, Yang HC, Li YC. Prediction of sepsis patients using machine learning approach: A meta-analysis. *Comput Methods Programs Biomed* 2019; **170**: 1-9 [PMID: 30712598 DOI: 10.1016/j.cmpb.2018.12.027]
28 **Zeynalova A**, Kocak B, Durmaz ES, Comunoglu N, Ozcan K, Ozcan G, Turk O, Tanriover N, Kocer N, Kizilkilic O, Islak C. Preoperative evaluation of tumour consistency in pituitary macroadenomas: a machine learning-based histogram analysis on conventional T2-weighted MRI. *Neuroradiology* 2019; **61**: 767-774 [PMID: 31011772 DOI: 10.1007/s00234-019-02211-2]
29 **Fan Y**, Hua M, Mou A, Wu M, Liu X, Bao X, Wang R, Feng M. Preoperative Noninvasive Radiomics Approach Predicts Tumor Consistency in Patients With Acromegaly: Development and Multicenter Prospective Validation. *Front Endocrinol (Lausanne)* 2019; **10**: 403 [PMID: 31316464 DOI: 10.3389/fendo.2019.00403]
30 **Niu J**, Zhang S, Ma S, Diao J, Zhou W, Tian J, Zang Y, Jia W. Preoperative prediction of cavernous sinus invasion by pituitary adenomas using a radiomics method based on magnetic resonance images. *Eur Radiol* 2019; **29**: 1625-1634 [PMID: 30255254 DOI: 10.1007/s00330-018-5725-3]
31 **Tamrazi B**, Pekmezci M, Aboian M, Tihan T, Glastonbury CM. Apparent diffusion coefficient and pituitary macroadenomas: pre-operative assessment of tumor atypia. *Pituitary* 2017; **20**: 195-200 [PMID: 27734275 DOI: 10.1007/s11102-016-0759-5]
32 **Ugga L**, Cuocolo R, Solari D, Guadagno E, D'Amico A, Somma T, Cappabianca P, Del Basso de Caro ML, Cavallo LM, Brunetti A. Prediction of high proliferative index in pituitary macroadenomas using MRI-based radiomics and machine learning. *Neuroradiology* 2019; **61**: 1365-1373 [PMID: 31375883 DOI: 10.1007/s00234-019-02266-1]
33 **Zhang S**, Song G, Zang Y, Jia J, Wang C, Li C, Tian J, Dong D, Zhang Y. Non-invasive radiomics approach potentially predicts non-functioning pituitary adenomas subtypes before surgery. *Eur Radiol* 2018; **28**: 3692-3701 [PMID: 29572634 DOI: 10.1007/s00330-017-5180-6]
34 **Heck A**, Emblem KE, Casar-Borota O, Bollerslev J, Ringstad G. Quantitative analyses of T2-weighted MRI as a potential marker for response to somatostatin analogs in newly diagnosed acromegaly. *Endocrine* 2016; **52**: 333-343 [PMID: 26475495 DOI: 10.1007/s12020-015-0766-8]
35 **Kocak B**, Durmaz ES, Kadioglu P, Polat Korkmaz O, Comunoglu N, Tanriover N, Kocer N, Islak C, Kizilkilic O. Predicting response to somatostatin analogues in acromegaly: machine learning-based high-dimensional quantitative texture analysis on T2-weighted MRI. *Eur Radiol* 2019; **29**: 2731-2739 [PMID: 30506213 DOI: 10.1007/s00330-018-5876-2]
36 **Lilja Y**, Gustafsson O, Ljungberg M, Starck G, Lindblom B, Skoglund T, Bergquist H, Jakobsson KE, Nilsson D. Visual pathway impairment by pituitary adenomas: quantitative diagnostics by diffusion tensor imaging. *J Neurosurg* 2017; **127**: 569-579 [PMID: 27885957 DOI: 10.3171/2016.8.JNS161290]
37 **Staartjes VE**, Serra C, Muscas G, Maldaner N, Akeret K, van Niftrik CHB, Fierstra J, Holzmann D, Regli L. Utility of deep neural networks in predicting gross-total resection after transsphenoidal surgery for pituitary adenoma: a pilot study. *Neurosurg Focus* 2018; **45**: E12 [PMID: 30453454 DOI: 10.3171/2018.8.FOCUS18243]

38 **Liu Y**, Liu X, Hong X, Liu P, Bao X, Yao Y, Xing B, Li Y, Huang Y, Zhu H, Lu L, Wang R, Feng M. Prediction of Recurrence after Transsphenoidal Surgery for Cushing's Disease: The Use of Machine Learning Algorithms. *Neuroendocrinology* 2019; **108**: 201-210 [PMID: 30630181 DOI: 10.1159/000496753]

39 **Staartjes VE**, Zattra CM, Akeret K, Maldaner N, Muscas G, Bas van Niftrik CH, Fierstra J, Regli L, Serra C. Neural network-based identification of patients at high risk for intraoperative cerebrospinal fluid leaks in endoscopic pituitary surgery. *J Neurosurg* 2019; 1-7 [PMID: 31226693 DOI: 10.3171/2019.4.JNS19477]

Artificial Intelligence in Medical Imaging

Submit a Manuscript: https://www.f6publishing.com

Artif Intell Med Imaging 2020 August 28; 1(2): 78-86

DOI: 10.35711/aimi.v1.i2.78

ISSN 2644-3260 (online)

MINIREVIEWS

Development of tomographic reconstruction for three-dimensional optical imaging: From the inversion of light propagation to artificial intelligence

Xin Cao, Kang Li, Xue-Li Xu, Karen M von Deneen, Guo-Hua Geng, Xue-Li Chen

ORCID number: Xin Cao 0000-0001-8658-8412; Kang Li 0000-0001-6218-5715; Xue-Li Xu 0000-0001-7518-376X; Karen M von Deneen 0000-0002-5310-1003; Guo-Hua Geng 0000-0003-2563-4029; Xue-Li Chen 0000-0002-3898-9892.

Author contributions: Cao X performed the majority of the writing and the investigation of articles; Li K and Xu XL performed the literature search and writing for the light propagation model-based OMT algorithm; Geng GH performed writing for the machine learning-based OMT algorithm; von Deneen KM polished the language and expression of the paper; Chen XL checked the organization and revised the writing of the paper.

Supported by the National Natural Science Foundation of China, No. 61701403; the Project Funded by China Post-doctoral Science Foundation, No. 2018M643719; the Young Talent Support Program of the Shaanxi Association for Science and Technology, No. 20190107; the Scientific Research Program Funded by Shaanxi Provincial Education Department, No. 18JK0767; and the Natural Science Research Plan Program in Shaanxi Province of China, No. 2017JQ6006.

Xin Cao, Kang Li, Xue-Li Xu, Guo-Hua Geng, School of Information Science and Technology, Northwest University, Xi'an 710069, Shaanxi Province, China

Karen M von Deneen, Xue-Li Chen, Engineering Research Center of Molecular and Neuro Imaging, Ministry of Education, and School of Life Science and Technology, Xidian University, Xi'an 710126, Shaanxi Province, China

Corresponding author: Xue-Li Chen, PhD, Professor, Engineering Research Center of Molecular and Neuro Imaging, Ministry of Education, and School of Life Science and Technology, Xidian University, No. 266 Xinglong Section of Xifeng Road, Xi'an 710126, Shaanxi Province, China. xlchen@xidian.edu.cn

Abstract

Optical molecular tomography (OMT) is an imaging modality which uses an optical signal, especially near-infrared light, to reconstruct the three-dimensional information of the light source in biological tissue. With the advantages of being low-cost, noninvasive and having high sensitivity, OMT has been applied in preclinical and clinical research. However, due to its serious ill-posedness and ill-condition, the solution of OMT requires heavy data analysis and the reconstruction quality is limited. Recently, the artificial intelligence (commonly known as AI)-based methods have been proposed to provide a different tool to solve the OMT problem. In this paper, we review the progress on OMT algorithms, from conventional methods to AI-based methods, and we also give a prospective towards future developments in this domain.

Key Words: Optical molecular tomography; Deep learning; Artificial intelligence; Light propagation based algorithm; Tomographic reconstruction

Core Tip: Most of the existing review articles about optical molecular tomography (OMT) focus on the traditional light propagation model-based algorithm, which possesses ill-posedness and ill-condition and the reconstruction result is unsatisfactory. The emergence of deep learning has brought OMT into the era of artificial intelligence, which can obtain a

Conflict-of-interest statement: The authors confirm having no conflict of interest in relation to this article's content.

Manuscript source: Invited manuscript

Received: June 5, 2020
Peer-review started: June 5, 2020
First decision: June 4, 2020
Revised: August 1, 2020
Accepted: August 22, 2020
Article in press: August 22, 2020
Published online: August 28, 2020

P-Reviewer: Nassar G, Ogino S
S-Editor: Wang JL
L-Editor: Filipodia
P-Editor: Xing YX

highly accurate reconstruction result. This article systematically reviews the development of tomographic reconstruction for OMT, which involves the light propagation model-based OMT algorithm and machine learning-based OMT algorithm. The challenges and perspectives of these machine learning-based algorithms are given at the end of the article.

Citation: Cao X, Li K, Xu XL, Deneen KMV, Geng GH, Chen XL. Development of tomographic reconstruction for three-dimensional optical imaging: From the inversion of light propagation to artificial intelligence. *Artif Intell Med Imaging* 2020; 1(2): 78-86
URL: https://www.wjgnet.com/2644-3260/full/v1/i2/78.htm
DOI: https://dx.doi.org/10.35711/aimi.v1.i2.78

INTRODUCTION

Optical molecular imaging (OMI) is the technology of using optical imaging instruments to detect biological tissues in organisms. In the time since Roger Yonchien Tsien reported that the tumor of a mouse could be resected under the guidance of fluorescence microscopy, winning the Nobel Prize in 2008, OMI has achieved rapid development, especially in recent years. With the advantages of high imaging sensitivity, tissue specificity, relatively short acquisition time and low cost, OMI has been successfully applied to many research fields, including - but not limited to - gene expression, tumor detection, drug development, and therapy evaluation[1-12]. However, OMI can only provide a two-dimensional image, which lacks deeper information and cannot describe the 3D distribution of the optical signal in an imaging object. Thus, researchers have proposed a series of 3D imaging methods, which can be named as optical molecular tomography (OMT).

In fact, OMT can be further divided into several subtypes, such as bioluminescence tomography, Cerenkov luminescence tomography (CLT), fluorescence molecular tomography (FMT), diffuse optical tomography, X-ray luminescence computed tomography (commonly referred to as XLCT), and so on[13-18]. The main difference between them is the means of producing the optical signal. For example, in CLT, the optical signal is emitted during the decay of a radionuclide probe, and in XLCT, high energy X-ray photons are used to excite X-ray excitable nanophosphors which emit the optical signal. Although the way of producing light signal varies, the reconstruction methods for these modalities can be concluded as one unified framework, as shown in Figure 1. It should be noted that anatomical information is essential for OMT, and in most cases, it is provided by X-ray computed tomography or magnetic resonance imaging[19-21]. Finally, the 3D distribution of the optical signal in the imaging object can be obtained, and the light source can then be located based on the reconstruction result. It is obvious that the core component of the framework is the OMT algorithm, which can determine the quality of the final reconstruction result.

In this review, we summarize recent progress on the OMT algorithm in two aspects: the traditional light propagation model-based way and machine learning-based way. Subsequently, we will provide a prospect towards future developments in a machine learning-based way for OMT.

LIGHT PROPAGATION MODEL-BASED OMT ALGORITHM

The accuracy of the traditional OMT algorithm is dependent on the description of photon propagation in biological tissue. The most popular light transfer model for OMT is the radiative transfer equation (RTE) from Maxwell's equations[22-25]. Although RTE can accurately depict photon propagation in diffusive media, it is a complicated integro-differential equation, and the computational time and memory requirements are extremely expensive. As a result, RTE is commonly simplified as the diffusion equation (DE, the lower-order approximation of the RTE)[26-28] and Nrd order is a simplified spherical harmonics function (SP3, the high-order approximation of RTE, and in most cases, N equals 3)[29-31]. After introducing the boundary condition, the simplified RTE can be solved using the finite element method[32-34] and the OMT problem can be linearized as the following weight matrix equation[28,25-37]: $AX = \Phi^{measure}$, where $X \geq 0$ (Eq. 1) "where A" denotes the optical transport system matrix, X is the unknown distribution of the optical source and $\Phi^{measure}$ represents the luminous flux of

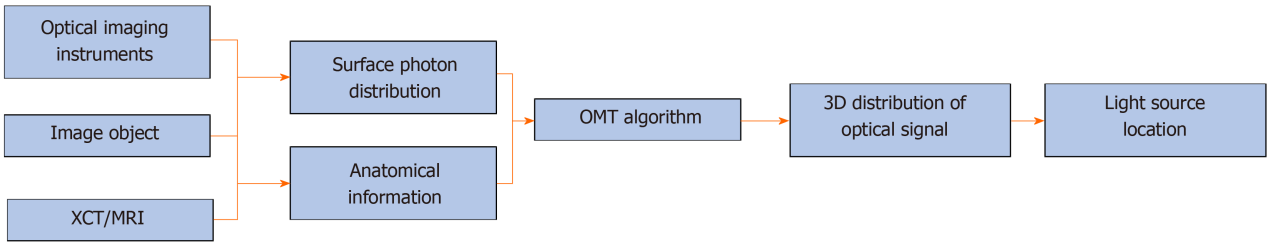

Figure 1 Main flowchart of optical molecular tomography. 3D: Three-dimensional; MRI: Magnetic resonance imaging; OMT: Optical molecular tomography; XCT: X-ray computed tomography.

the vertices. As $\Phi^{measure}$ can only be collected on the surface of an imaging object, the goal of OMT can be regarded as the determination of the 3D luminescence source distribution X from boundary measurements $\Phi^{measure}$ based on the formulation of Eq. 1, and this is a typically inverse problem. It should be noted that the number of measurements is often substantially less than the number of unknowns, making the inverse reconstruction an ill-conditioned problem.

Up until now, many methods have been developed to address the limitation mentioned above to make the OMT algorithm strong and robust. These methods can be roughly divided into two categories. The first one is the priori information-based method. In these methods, *a priori* information is first inferred according to the surface light power distribution and the heterogeneous structure of the imaging object, and then is used as the permissible source region. The aim of using *a priori* information is to constrain the unknown sources in the region where the sources may exist, resulting in the reduction of the amount of unknown source locations. Many numerical and *in vivo* experiments have been conducted, and the results indicate that the size of the permissible source region can significantly affect the reconstruction quality[37-46]. It is obvious that the smaller the permissible source region, the more stable the reconstruction results. The main obstacle of the priori information-based methods is that the prior information about the permissible source region cannot always be obtained in advance, especially for the early diseased tissue which cannot be distinguished from anatomical information. Figure 2 shows the reconstruction results with *a priori* information[47].

The second one is the posteriori information-based method. In these methods, the whole object is used as the initial permissible source region, and the permissible region is updated by selecting the elements where the reconstructed energy is relatively higher than others[48-53]. As the posteriori information-based method avoids the segmentation of the permissible source region from anatomical information, it has superior generalization performance than the priori information-based method, and most of the recent studies are focused on optimizing it[54-58]. Besides the above methods for OMT, the reconstruction accuracy can also be improved by increasing the number of detectable measurements[46,59-66]. For example, in FMT, the quality of the reconstructed results can be improved with the increasing number of measurement data. In CLT, multispectral images can be acquired using a group of filters and the result can be improved significantly. The drawback of this method is that the more optical signal data are acquired, the more time is consumed. However, these traditional light propagation model-based methods are still limited to their reconstruction accuracy, and the main reason is that the simplified RTE cannot accurately describe the process of photon propagation. Thus, more effective methods to improve the reconstruction quality of OMT are still required. Figure 3 shows the reconstruction results with posteriori information[62,67].

MACHINE LEARNING-BASED OMT ALGORITHM

With the development of artificial intelligence (AI), machine learning algorithms, especially deep learning-based technologies, have gained stunning successes at solving difficult and previously unsolved computational problems in many fields, such as computer vision, natural language processing, speech recognition, and so on[68-71]. The great success of AI has also attracted the attention of researchers in the field of OMT. Based on multilayer perceptrons (commonly known as MLPs), Gao *et al*[72] proposed a data-driven-based strategy for OMT. As the machine learning-based method requires

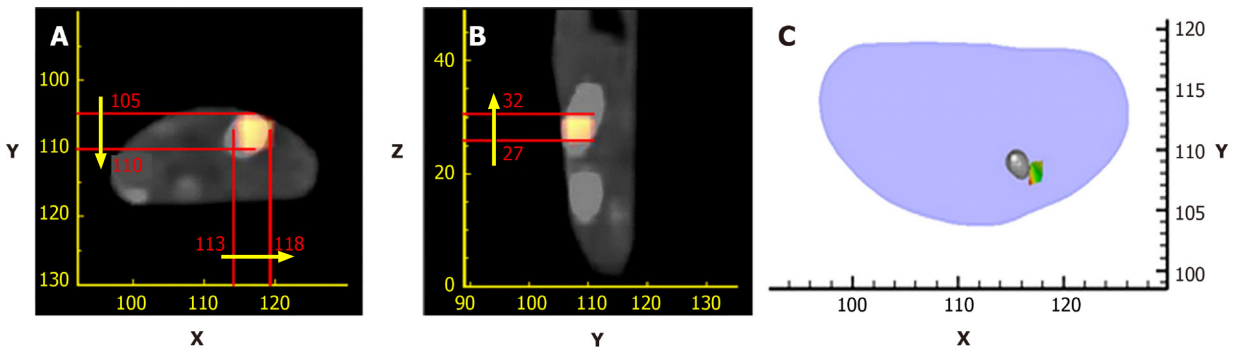

Figure 2 Reconstruction results with *a priori* information. A and B: The axial and sagittal views of single photon emission computed tomography/computed tomography imaging, and an implanted light source is inserted into a mouse; C: The axial-view result of the reconstructed source. These images are reproduced from[47].

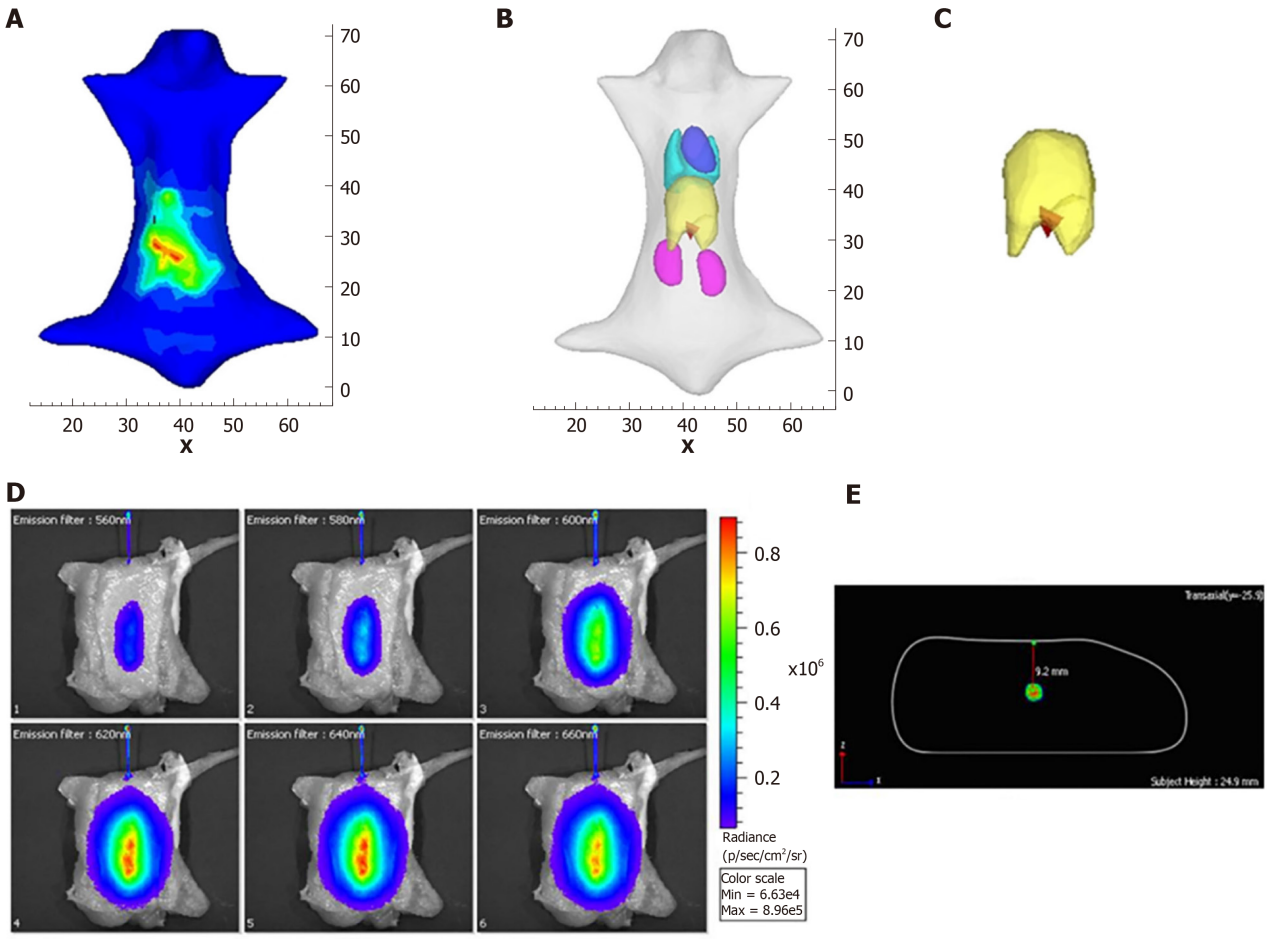

Figure 3 Reconstruction results with posteriori information. A: The luminescence distribution in the body; B and C: The three-dimensional results and the results of the local enlarged image in the local area of the liver; C: The images of the capillary acquired using six filters; D, E: The trans-axial multispectral-Cerenkov luminescence tomography reconstructed image of the capillary filled with ^{32}P-ATP at a 9 mm depth. A and B are reproduced from[67], while C and D are reproduced from[62].

large amounts of data to train the network, Molecular Optical Simulation Environment software[73] is adopted to produce the simulation data. The experimental results showed the proposed method can greatly improve the reconstruction quality compared with conventional approaches. Subsequently, based on the convolutional neural network and recurrent neural network, Guo *et al*[74] proposed a framework for FMT reconstruction. The input of this method is two-dimensional fluorescent images, which can avoid errors caused by mesh registration in conventional methods. Zhang *et al*[75] used MLPs to solve the CLT problem, and the complex relationship between the

surface optical signal and the true photon source has been learned by the network. Meng *et al*[76] constructed a K-nearest neighbor-based locally connected network (KNN-LCN) for FMT. In their work, KNN-LCN cascades a fully connected (referred to as FC) sub-network with a locally connected (referred to as LC) sub-network, where the FC part provides a coarse reconstruction result and the LC part fine-tunes the morphological quality of the reconstructed result. Compared to the traditional light propagation model-based methods, the biggest advantage of the machine learning-based method is that it can directly fit the nonlinear relationship between an object surface optical density and its internal luminescence source. Figure 4 shows the structure of the networks used in OMT reconstruction[72,74-76].

CONCLUSION

Although the machine learning-based OMT algorithm can obtain a more accurate reconstruction result than the traditional light propagation model-based algorithm, further application is still limited and requires more theoretical research. One reason is that the network trained for one object cannot be used for others, and if the object is changed, another network with different parameters should be built and its training will cost a lot of time. Another reason is that there is no ideal method that can explain the mechanism of such a neural network. The solution to the above two limitations is the development direction for future research. In addition, there are many environmental, dietary, and other factors that influence the microbiome, immune system, and pathogenic mechanisms. The recent studies on molecular pathological epidemiology have provided a powerful tool which can pathologically, epidemiologically investigate those factors in relation to molecular pathologies, immunity, and clinical outcomes[77], and it is believed that the molecular pathological epidemiology research can be a promising direction and in which OMT can take a big role.

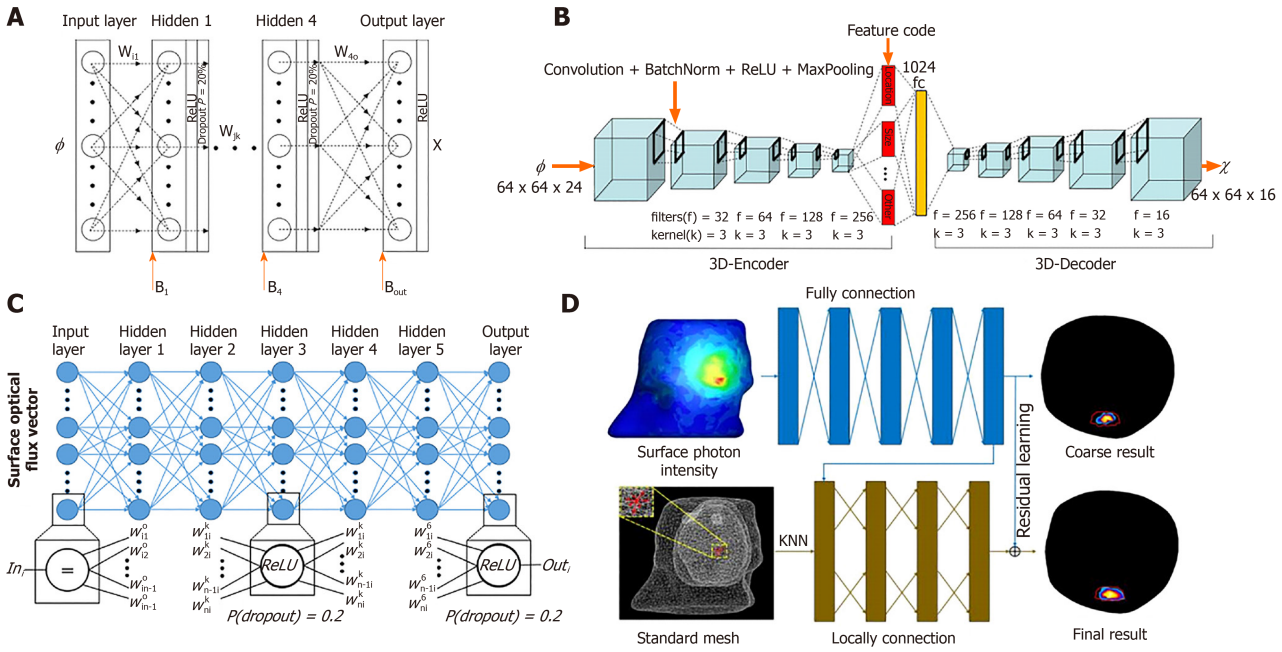

Figure 4 Structure of the networks used in optical molecular tomography reconstruction. A: Multilayer perceptron-based bioluminescence tomography reconstruction network reproduced from[72]; B: Convolutional neural network-recurrent neural network-based fluorescence molecular tomography (FMT) reconstruction framework reproduced from[74]; C: Multilayer fully-connected neural network based on Cerenkov luminescence tomography reproduced from[75]; D: K-nearest neighbor-based locally connected network based on FMT reproduced from[76].

REFERENCES

1 **Weissleder R**, Pittet MJ. Imaging in the era of molecular oncology. *Nature* 2008; **452**: 580-589 [PMID: 18385732 DOI: 10.1038/nature06917]

2 **Nguyen QT**, Tsien RY. Fluorescence-guided surgery with live molecular navigation--a new cutting edge. *Nat Rev Cancer* 2013; **13**: 653-662 [PMID: 23924645 DOI: 10.1038/nrc3566]

3 **Hu Z**, Qu Y, Wang K, Zhang X, Zha J, Song T, Bao C, Liu H, Wang Z, Wang J, Liu Z, Liu H, Tian J. In vivo nanoparticle-mediated radiopharmaceutical-excited fluorescence molecular imaging. *Nat Commun* 2015; **6**: 7560 [PMID: 26123615 DOI: 10.1038/ncomms8560]

4 **Klose AD**, Paragas N. Automated quantification of bioluminescence images. *Nat Commun* 2018; **9**: 4262 [PMID: 30323260 DOI: 10.1038/s41467-018-06288-w]

5 **Thorek DL**, Ogirala A, Beattie BJ, Grimm J. Quantitative imaging of disease signatures through radioactive decay signal conversion. *Nat Med* 2013; **19**: 1345-1350 [PMID: 24013701 DOI: 10.1038/nm.3323]

6 **Zhang Z**, Cai M, Bao C, Hu Z, Tian J. Endoscopic Cerenkov luminescence imaging and image-guided tumor resection on hepatocellular carcinoma-bearing mouse models. *Nanomedicine* 2019; **17**: 62-70 [PMID: 30654183 DOI: 10.1016/j.nano.2018.12.017]

7 **Mitchell GS**, Lloyd PNT, Cherry SR. Cerenkov luminescence and PET imaging of ^{90}Y: capabilities and limitations in small animal applications. *Phys Med Biol* 2020; **65**: 065006 [PMID: 32045899 DOI: 10.1088/1361-6560/ab7502]

8 **Cao X**, Zhan Y, Cao X, Liang J, Chen X. Harnessing the Power of Cerenkov Luminescence Imaging for Gastroenterology: Cerenkov Luminescence Endoscopy. *Curr Med Imaging Rev* 2017; **13**: 50-57 [DOI: 10.2174/1573405612666160607094334]

9 **Cao X**, Chen X, Kang F, Zhan Y, Cao X, Wang J, Liang J, Tian J. Intensity Enhanced Cerenkov Luminescence Imaging Using Terbium-Doped Gd2O2S Microparticles. *ACS Appl Mater Interfaces* 2015; **7**: 11775-11782 [PMID: 25992597 DOI: 10.1021/acsami.5b00432]

10 **Cao X**, Chen X, Kang F, Cao X, Zhan Y, Wang J, Wu K, Liang J. Sensitivity improvement of Cerenkov luminescence endoscope with terbium doped Gd2O2S nanoparticles. *Appl Phys Lett* 2015; **106**: 4 [DOI: 10.1063/1.4921858]

11 **Cao X**, Chen X, Kang F, Lin Y, Liu M, Hu H, Nie Y, Wu K, Wang J, Liang J, Tian J. Performance evaluation of endoscopic Cerenkov luminescence imaging system: in vitro and pseudotumor studies. *Biomed Opt Express* 2014; **5**: 3660-3670 [PMID: 25360380 DOI: 10.1364/BOE.5.003660]

12 **Fan D**, Zhang X, Zhong L, Liu X, Sun Y, Zhao H, Jia B, Liu Z, Zhu Z, Shi J, Wang F. (68)Ga-labeled 3PRGD2 for dual PET and Cerenkov luminescence imaging of orthotopic human glioblastoma. *Bioconjug Chem* 2015; **26**: 1054-1060 [PMID: 25853280 DOI: 10.1021/acs.bioconjchem.5b00169]

13 **Gao Y**, Wang K, Jiang S, Liu Y, Ai T, Tian J. Corrections to "Bioluminescence Tomography Based on Gaussian Weighted Laplace Prior Regularization for Morphological Imaging of Glioma". *IEEE Trans Med Imaging* 2018; **37**: 1733 [PMID: 29969423 DOI: 10.1109/TMI.2018.2845038]

14 **Zhong J**, Qin C, Yang X, Zhu S, Zhang X, Tian J. Cerenkov luminescence tomography for in vivo radiopharmaceutical imaging. *Int J Biomed Imaging* 2011; **2011**: 641618 [PMID: 21747821 DOI: 10.1155/2011/641618]

15 **Zhang B**, Liu S, Cao X, Liu F, Wang X, Luo J, Shan B, Bai J. Fluorescence Tomography Reconstruction

With Simultaneous Positron Emission Tomography Priors. *IEEE Trans Multimedia* 2013; **15**: 1031-1038 [DOI: 10.1109/TMM.2013.2244205]

16 **Baritaux JC**, Hassler K, Bucher M, Sanyal S, Unser M. Sparsity-driven reconstruction for FDOT with anatomical priors. *IEEE Trans Med Imaging* 2011; **30**: 1143-1153 [PMID: 21507771 DOI: 10.1109/TMI.2011.2136438]

17 **Lewis MA**, Kodibagkar VD, Öz OK, Mason RP. On the potential for molecular imaging with Cerenkov luminescence. *Opt Lett* 2010; **35**: 3889-3891 [PMID: 21124555 DOI: 10.1364/OL.35.003889]

18 **Contag CH**, Bachmann MH. Advances in in vivo bioluminescence imaging of gene expression. *Annu Rev Biomed Eng* 2002; **4**: 235-260 [PMID: 12117758 DOI: 10.1146/annurev.bioeng.4.111901.093336]

19 **Meng H**, Wang K, Gao Y, Jin Y, Ma X, Tian J. Adaptive Gaussian Weighted Laplace Prior Regularization Enables Accurate Morphological Reconstruction in Fluorescence Molecular Tomography. *IEEE Trans Med Imaging* 2019; **38**: 2726-2734 [PMID: 31021763 DOI: 10.1109/TMI.2019.2912222]

20 **Guo H**, Hou Y, He X, Yu J, Cheng J, Pu X. Adaptive hp finite element method for fluorescence molecular tomography with simplified spherical harmonics approximation. *J Innov Opt Health Sci* 2014; **7**: 12 [DOI: 10.1142/S1793545813500570]

21 **Yi H**, Wei H, Peng J, Hou Y, He X. Adaptive threshold method for recovered images of FMT. *J Opt Soc Am A Opt Image Sci Vis* 2018; **35**: 256-261 [PMID: 29400892 DOI: 10.1364/JOSAA.35.000256]

22 **Cai W**, Xu M, Alfano R. Three-dimensional radiative transfer tomography for turbid media. *IEEE J Sel Top Quantum Electron* 2003; **9**: 189-198 [DOI: 10.1109/JSTQE.2003.813312]

23 **Joshi A**, Rasmussen JC, Sevick-Muraca EM, Wareing TA, McGhee J. Radiative transport-based frequency-domain fluorescence tomography. *Phys Med Biol* 2008; **53**: 2069-2088 [PMID: 18364555 DOI: 10.1088/0031-9155/53/8/005]

24 **Gao H**, Zhao H. Multilevel bioluminescence tomography based on radiative transfer equation Part 1: l1 regularization. *Opt Express* 2010; **18**: 1854-1871 [PMID: 20174013 DOI: 10.1364/OE.18.001854]

25 **Klose AD**. The forward and inverse problem in tissue optics based on the radiative transfer equation: a brief review. *J Quant Spectrosc Radiat Transf* 2010; **111**: 1852-1853 [PMID: 20607145 DOI: 10.1016/j.jqsrt.2010.01.020]

26 **Wang G**, Cong W, Durairaj K, Qian X, Shen H, Sinn P, Hoffman E, McLennan G, Henry M. In vivo mouse studies with bioluminescence tomography. *Opt Express* 2006; **14**: 7801-7809 [PMID: 19529149 DOI: 10.1364/OE.14.007801]

27 **Cong W**, Wang G, Kumar D, Liu Y, Jiang M, Wang L, Hoffman E, McLennan G, McCray P, Zabner J, Cong A. Practical reconstruction method for bioluminescence tomography. *Opt Express* 2005; **13**: 6756-6771 [PMID: 19498692 DOI: 10.1364/OPEX.13.006756]

28 **Li C**, Mitchell GS, Cherry SR. Cerenkov luminescence tomography for small-animal imaging. *Opt Lett* 2010; **35**: 1109-1111 [PMID: 20364233 DOI: 10.1364/OL.35.001109]

29 **Yang D**, Chen X, Cao X, Wang J, Liang J, Tian J. Performance investigation of SP3 and diffusion approximation for three-dimensional whole-body optical imaging of small animals. *Med Biol Eng Comput* 2015; **53**: 805-814 [PMID: 25850985 DOI: 10.1007/s11517-015-1293-8]

30 **Zhong J**, Tian J, Yang X, Qin C. Whole-body Cerenkov luminescence tomography with the finite element SP(3) method. *Ann Biomed Eng* 2011; **39**: 1728-1735 [PMID: 21301961 DOI: 10.1007/s10439-011-0261-1]

31 **Zhong J**, Tian J, Yang X, Qin C. L1-regularized Cerenkov luminescence tomography with a SP3 method and CT fusion. *Conf Proc IEEE Eng Med Biol Soc* 2011; **2011**: 6158-6161 [PMID: 22255745 DOI: 10.1109/IEMBS.2011.6091521]

32 **Han D**, Tian J, Zhu S, Feng J, Qin C, Zhang B, Yang X. A fast reconstruction algorithm for fluorescence molecular tomography with sparsity regularization. *Opt Express* 2010; **18**: 8630-8646 [PMID: 20588707 DOI: 10.1364/OE.18.008630]

33 **Chen X**, Gao X, Chen D, Ma X, Zhao X, Shen M, Li X, Qu X, Liang J, Ripoll J, Tian J. 3D reconstruction of light flux distribution on arbitrary surfaces from 2D multi-photographic images. *Opt Express* 2010; **18**: 19876-19893 [PMID: 20940879 DOI: 10.1364/OE.18.019876]

34 **Han R**, Liang J, Qu X, Hou Y, Ren N, Mao J, Tian J. A source reconstruction algorithm based on adaptive hp-FEM for bioluminescence tomography. *Opt Express* 2009; **17**: 14481-14494 [PMID: 19687926 DOI: 10.1364/OE.17.014481]

35 **Lu Y**, Zhu B, Shen H, Rasmussen JC, Wang G, Sevick-Muraca EM. A parallel adaptive finite element simplified spherical harmonics approximation solver for frequency domain fluorescence molecular imaging. *Phys Med Biol* 2010; **55**: 4625-4645 [PMID: 20671350 DOI: 10.1088/0031-9155/55/16/002]

36 **Liu K**, Lu Y, Tian J, Qin C, Yang X, Zhu S, Yang X, Gao Q, Han D. Evaluation of the simplified spherical harmonics approximation in bioluminescence tomography through heterogeneous mouse models. *Opt Express* 2010; **18**: 20988-21002 [PMID: 20940994 DOI: 10.1364/OE.18.020988]

37 **Liu J**, Wang Y, Qu X, Li X, Ma X, Han R, Hu Z, Chen X, Sun D, Zhang R, Chen D, Chen D, Chen X, Liang J, Cao F, Tian J. In vivo quantitative bioluminescence tomography using heterogeneous and homogeneous mouse models. *Opt Express* 2010; **18**: 13102-13113 [PMID: 20588440 DOI: 10.1364/OE.18.013102]

38 **Baikejiang R**, Zhao Y, Fite BZ, Ferrara KW, Li C. Anatomical image-guided fluorescence molecular tomography reconstruction using kernel method. *J Biomed Opt* 2017; **22**: 55001 [PMID: 28464120 DOI: 10.1117/1.JBO.22.5.055001]

39 **Holt RW**, Demers JL, Sexton KJ, Gunn JR, Davis SC, Samkoe KS, Pogue BW. Tomography of epidermal growth factor receptor binding to fluorescent Affibody in vivo studied with magnetic resonance guided fluorescence recovery in varying orthotopic glioma sizes. *J Biomed Opt* 2015; **20**: 26001 [PMID: 25652703 DOI: 10.1117/1.JBO.20.2.026001]

40 **Davis SC**, Samkoe KS, Tichauer KM, Sexton KJ, Gunn JR, Deharvengt SJ, Hasan T, Pogue BW. Dynamic dual-tracer MRI-guided fluorescence tomography to quantify receptor density in vivo. *Proc Natl Acad Sci U S A* 2013; **110**: 9025-9030 [PMID: 23671066 DOI: 10.1073/pnas.1213490110]

41 **Qin C**, Zhu S, Feng J, Zhong J, Ma X, Wu P, Tian J. Comparison of permissible source region and multispectral data using efficient bioluminescence tomography method. *J Biophotonics* 2011; **4**: 824-839 [PMID: 21987294 DOI: 10.1002/jbio.201100049]

42 **Ma X**, Tian J, Qin C, Yang X, Zhang B, Xue Z, Zhang X, Han D, Dong D, Liu X. Early detection of liver

cancer based on bioluminescence tomography. *Appl Opt* 2011; **50**: 1389-1395 [PMID: 21460905 DOI: 10.1364/AO.50.001389]

43 **Huang H**, Qu X, Liang J, He X, Chen X, Yang D, Tian J. A multi-phase level set framework for source reconstruction in bioluminescence tomography. *J Comput Phys* 2010; **229**: 5246-5256 [DOI: 10.1016/j.jcp.2010.03.041]

44 **Davis SC**, Samkoe KS, O'Hara JA, Gibbs-Strauss SL, Paulsen KD, Pogue BW. Comparing implementations of magnetic-resonance-guided fluorescence molecular tomography for diagnostic classification of brain tumors. *J Biomed Opt* 2010; **15**: 051602 [PMID: 21054076 DOI: 10.1117/1.3483902]

45 **Schulz RB**, Ale A, Sarantopoulos A, Freyer M, Soehngen E, Zientkowska M, Ntziachristos V. Hybrid system for simultaneous fluorescence and x-ray computed tomography. *IEEE Trans Med Imaging* 2010; **29**: 465-473 [PMID: 19906585 DOI: 10.1109/TMI.2009.2035310]

46 **Feng J**, Jia K, Yan G, Zhu S, Qin C, Lv Y, Tian J. An optimal permissible source region strategy for multispectral bioluminescence tomography. *Opt Express* 2008; **16**: 15640-15654 [PMID: 18825203 DOI: 10.1364/OE.16.015640]

47 **Hu Z**, Chen X, Liang J, Qu X, Chen D, Yang W, Wang J, Cao F, Tian J. Single photon emission computed tomography-guided Cerenkov luminescence tomography. *J Appl Phys* 2012; **112**: 024703 [DOI: 10.1063/1.4739266]

48 **Chehade M**, Srivastava AK, Bulte JW. Co-Registration of Bioluminescence Tomography, Computed Tomography, and Magnetic Resonance Imaging for Multimodal *In Vivo* Stem Cell Tracking. *Tomography* 2016; **2**: 159-165 [PMID: 27478872 DOI: 10.18383/j.tom.2016.00160]

49 **Zhang X**, Lu Y, Chan T. A novel sparsity reconstruction method from Poisson data for 3D bioluminescence tomography. *J Sci Comput* 2012; **50**: 519-535 [DOI: 10.1007/s10915-011-9533-z]

50 **Dutta J**, Ahn S, Li C, Cherry SR, Leahy RM. Joint L1 and total variation regularization for fluorescence molecular tomography. *Phys Med Biol* 2012; **57**: 1459-1476 [PMID: 22390906 DOI: 10.1088/0031-9155/57/6/1459]

51 **Liu K**, Tian J, Qin C, Yang X, Zhu S, Han D, Wu P. Tomographic bioluminescence imaging reconstruction via a dynamically sparse regularized global method in mouse models. *J Biomed Opt* 2011; **16**: 046016 [PMID: 21529085 DOI: 10.1117/1.3570828]

52 **Lu Y**, Zhang X, Douraghy A, Stout D, Tian J, Chan TF, Chatziioannou AF. Source reconstruction for spectrally-resolved bioluminescence tomography with sparse a priori information. *Opt Express* 2009; **17**: 8062-8080 [PMID: 19434138 DOI: 10.1364/OE.17.008062]

53 **Xu X**, Deng Z, Iordachita I, Wong J, Wang K. A Novel Multi-Projection Bioluminescence Tomography for Small Animal Radiation Research Platform (SARRP). *Med Phys* 2018; **45**: E393-E393

54 **Guo H**, Gao L, Yu J, He X, Wang H, Zheng J, Yang X. Sparse-graph manifold learning method for bioluminescence tomography. *J Biophotonics* 2020; **13**: e201960218 [PMID: 31990430 DOI: 10.1002/jbio.201960218]

55 **Cai M**, Zhang Z, Shi X, Yang J, Hu Z, Tian J. Non-negative Iterative Convex Refinement Approach for Accurate and Robust Reconstruction in Cerenkov Luminescence Tomography. *IEEE Trans Med Imaging* 2020 [PMID: 32324543 DOI: 10.1109/TMI.2020.2987640]

56 **Wang L**, Cao H, Cao X, Ren S, Li K, Zhan Y, Chen X, He X. Adaptively Hybrid 3 Simplified Spherical Harmonics With Diffusion Equation-Based Multispectral Cerenkov Luminescence Tomography. *IEEE Access* 2019; **7**: 160779-160785 [DOI: 10.1109/ACCESS.2019.2950265]

57 **Pu H**, Gao P, Liu Y, Rong J, Shi F, Lu H. Principal Component Analysis Based Dynamic Cone Beam X-Ray Luminescence Computed Tomography: A Feasibility Study. *IEEE Trans Med Imaging* 2019; **38**: 2891-2902 [PMID: 31095480 DOI: 10.1109/TMI.2019.2917026]

58 **Liu X**, Tang X, Shu Y, Zhao L, Liu Y, Zhou T. Single-view cone-beam x-ray luminescence optical tomography based on Group_YALL1 method. *Phys Med Biol* 2019; **64**: 105004 [PMID: 30970336 DOI: 10.1088/1361-6560/ab1819]

59 **He X**, Xiang W, Yu J, Li Q. Penalty method for source reconstruction of multispectral bioluminescence tomography. *Opt Eng* 2018; **57**: 083104 [DOI: 10.1117/1.OE.57.8.083104]

60 **Guo H**, He X, Liu M, Zhang Z, Hu Z, Tian J. Weight Multispectral Reconstruction Strategy for Enhanced Reconstruction Accuracy and Stability With Cerenkov Luminescence Tomography. *IEEE Trans Med Imaging* 2017; **36**: 1337-1346 [PMID: 28182554 DOI: 10.1109/TMI.2017.2658661]

61 **Liu H**, Yang X, Song T, Bao C, Shi L, Hu Z, Wang K, Tian J. Multispectral hybrid Cerenkov luminescence tomography based on the finite element SPn method. *J Biomed Opt* 2015; **20**: 86007 [PMID: 26271053 DOI: 10.1117/1.JBO.20.8.086007]

62 **Spinelli AE**, Kuo C, Rice BW, Calandrino R, Marzola P, Sbarbati A, Boschi F. Multispectral Cerenkov luminescence tomography for small animal optical imaging. *Opt Express* 2011; **19**: 12605-12618 [PMID: 21716501 DOI: 10.1364/OE.19.012605]

63 **Li C**, Yang Y, Mitchell GS, Cherry SR. Simultaneous PET and multispectral 3-dimensional fluorescence optical tomography imaging system. *J Nucl Med* 2011; **52**: 1268-1275 [PMID: 21810591 DOI: 10.2967/jnumed.110.082859]

64 **Crane LM**, Themelis G, Pleijhuis RG, Harlaar NJ, Sarantopoulos A, Arts HJ, van der Zee AG, Ntziachristos V, van Dam GM. Intraoperative multispectral fluorescence imaging for the detection of the sentinel lymph node in cervical cancer: a novel concept. *Mol Imaging Biol* 2011; **13**: 1043-1049 [PMID: 20835767 DOI: 10.1007/s11307-010-0425-7]

65 **Chaudhari AJ**, Darvas F, Bading JR, Moats RA, Conti PS, Smith DJ, Cherry SR, Leahy RM. Hyperspectral and multispectral bioluminescence optical tomography for small animal imaging. *Phys Med Biol* 2005; **50**: 5421-5441 [PMID: 16306643 DOI: 10.1088/0031-9155/50/23/001]

66 **Tong S**, Han B, Chen Y, Tang J, Bi B, Gu R. RTE-based parameter reconstruction with TV+L1 regularization. *J Comput Appl Math* 2018; **337**: 256-273 [DOI: 10.1016/j.cam.2018.01.011]

67 **Yang D**, Wang L, Chen D, Yan C, He X, Liang J, Chen X. Filtered maximum likelihood expectation maximization based global reconstruction for bioluminescence tomography. *Med Biol Eng Comput* 2018; **56**: 2067-2081 [PMID: 29770920 DOI: 10.1007/s11517-018-1842-z]

68 **Gurovich Y**, Hanani Y, Bar O, Nadav G, Fleischer N, Gelbman D, Basel-Salmon L, Krawitz PM,

Kamphausen SB, Zenker M, Bird LM, Gripp KW. Identifying facial phenotypes of genetic disorders using deep learning. *Nat Med* 2019; **25**: 60-64 [PMID: 30617323 DOI: 10.1038/s41591-018-0279-0]

69 **Hannun AY**, Rajpurkar P, Haghpanahi M, Tison GH, Bourn C, Turakhia MP, Ng AY. Cardiologist-level arrhythmia detection and classification in ambulatory electrocardiograms using a deep neural network. *Nat Med* 2019; **25**: 65-69 [PMID: 30617320 DOI: 10.1038/s41591-018-0268-3]

70 **Moen E**, Bannon D, Kudo T, Graf W, Covert M, Van Valen D. Deep learning for cellular image analysis. *Nat Methods* 2019; **16**: 1233-1246 [PMID: 31133758 DOI: 10.1038/s41592-019-0403-1]

71 **LeCun Y**, Bengio Y, Hinton G. Deep learning. *Nature* 2015; **521**: 436-444 [PMID: 26017442 DOI: 10.1038/nature14539]

72 **Gao Y**, Wang K, An Y, Jiang S, Meng H, Tian J. Nonmodel-based bioluminescence tomography using a machine-learning reconstruction strategy. *Optica* 2018; **5**: 1451-1454 [DOI: 10.1364/OPTICA.5.001451]

73 **Ren S**, Chen X, Wang H, Qu X, Wang G, Liang J, Tian J. Molecular Optical Simulation Environment (MOSE): a platform for the simulation of light propagation in turbid media. *PLoS One* 2013; **8**: e61304 [PMID: 23577215 DOI: 10.1371/journal.pone.0061304]

74 **Guo L**, Liu F, Cai C, Liu J, Zhang G. 3D deep encoder-decoder network for fluorescence molecular tomography. *Opt Lett* 2019; **44**: 1892-1895 [PMID: 30985768 DOI: 10.1364/OL.44.001892]

75 **Zhang Z**, Cai M, Gao Y, Shi X, Zhang X, Hu Z, Tian J. A novel Cerenkov luminescence tomography approach using multilayer fully connected neural network. *Phys Med Biol* 2019; **64**: 245010 [PMID: 31770734 DOI: 10.1088/1361-6560/ab5bb4]

76 **Meng H**, Gao Y, Yang X, Wang K, Tian J. K-nearest Neighbor Based Locally Connected Network for Fast Morphological Reconstruction in Fluorescence Molecular Tomography. *IEEE Trans Med Imaging* 2020 [PMID: 32286961 DOI: 10.1109/TMI.2020.2984557]

77 **Ogino S**, Lochhead P, Chan AT, Nishihara R, Cho E, Wolpin BM, Meyerhardt JA, Meissner A, Schernhammer ES, Fuchs CS, Giovannucci E. Molecular pathological epidemiology of epigenetics: emerging integrative science to analyze environment, host, and disease. *Mod Pathol* 2013; **26**: 465-484 [PMID: 23307060 DOI: 10.1038/modpathol.2012.214]

Published by **Baishideng Publishing Group Inc**
7041 Koll Center Parkway, Suite 160, Pleasanton, CA 94566, USA
Telephone: +1-925-3991568
E-mail: bpgoffice@wjgnet.com
Help Desk: https://www.f6publishing.com/helpdesk
https://www.wjgnet.com